

Consolidation of a clay layer overlying a smooth-rigid base due to surface loads

MANOJ PURI

Department of Mathematics, Guru Jambheshwar University of Science
and Technology, Hisar-125001, India.
E-mail: mnj243puri@gmail.com

SUNITA RANI*

Department of Mathematics, Guru Jambheshwar University of Science
and Technology, Hisar-125001, India.
E-mail: s_b_rani@rediffmail.com

Abstract

The solution of coupled system of equations governing the diffusion-deformation of a poroelastic media for the plane strain case is used to obtain the settlement of a clay layer overlying a smooth-rigid permeable or impermeable base. Both the fluid as well as solid constituents are compressible and the permeability is taken to be anisotropic. The solution is obtained in the Laplace-Fourier transform domain. Explicit expressions for the displacements, stresses and the pore pressure have been obtained for the normal strip and normal line loading. For numerical computations, we assume the poroelastic layer is of Indiana Limestone. The consolidation of the layer is computed in the space time domain for the normal strip loading. Numerical results reveal that permeability of the base has a significant effect on the surface settlement for a thin layer. Contour maps showing the diffusion of pore pressure in the layer have been plotted for the normal strip and normal line loading. The pore pressure vanishes more rapidly for the permeable base as compared to the impermeable base.

Mathematics Subject Classification: 74F10;76S05

Keywords. Plane strain, poroelastic, compressible constituents, anisotropic permeability, normal strip loading, Normal line loading.

1. Introduction

Biot's theory of linear poroelasticity has been used extensively to study the consolidation of poroelastic layer e.g. Gibson *et al.* [1], Booker [2], Booker and Small [3], Yue & Selvadurai [4], Barry *et al.* [5], Chen [6], Chen *et al.* [7,8], Ai & Wang [9], Singh *et al.* [10], Ai *et al.* [11], Rani *et al.* [12], Ai *et al.* [13], Rani *et al.* [14] etc.. In most of these studies, the layer rests on a rough rigid pervious or impervious base. There are very few studies in the literature in which the layer rests upon a smooth rigid base e.g. Gibson *et al.* [7], Rani and Rani [15].

Gibson *et al.* [1] obtained the plane strain and axially symmetric consolidation of a clay layer resting upon a smooth rigid base due to circular or strip loading assuming the fluid as well as solid constituents incompressible. Booker [2] solved the problem of the consolidation of a finite clay layer upon a rough-rigid base subjected to general surface loading, assuming the pore fluid to be incompressible. Chen *et al.* [7,8] discussed axisymmetric consolidation of soil layer on a rough impermeable base subjected to a uniform circular pressure at the ground surface. The layer is transversely isotropic in its elastic and hydraulic properties. Ai and Wang [9] studied the axisymmetric deformation of a finite soil stratum with incompressible solid and fluid components using Laplace and Hankel transforms in terms of elements of Thomson Haskell matrix. Rani *et al.* [12] obtained the deformation of a poroelastic clay layer with anisotropic permeability overlying a rough-rigid impermeable base due to axisymmetric normal loading. They assumed the fluid and solid components compressible. Rani *et al.* [14] extended the solution in the Cartesian form assuming the layer overlying a rough rigid permeable or impermeable base and showed that the permeability of the base accelerates the consolidation process.

In the present paper, we generalize the solution obtained by Gibson *et al.* [1] for the plane strain consolidation of a clay layer overlying a smooth rigid base subjected to normal strip and normal line loading assuming the fluid as well as solid constituents compressible and the hydraulic permeability to be anisotropic. We formulate the plane strain deformation of a clay layer resting on a smooth rigid permeable or impermeable base due to surface loads using the Biot's stress function approach. The expressions for the displacements, stresses and the pore pressure are obtained in the Laplace Fourier domain by applying the suitable boundary conditions. Explicit expressions for the consolidation and the pore pressure have been obtained at any arbitrary point of the layer for the normal strip loading. The double integral is evaluated numerically to obtain the solution in the space-time domain. The Laplace inversion has been solved by using Talbot's algorithm and the Fourier integral by extended Simpson's formula. The effect of anisotropic in permeability and the compressibilities of solid/fluid constituents on the consolidation has been studied numerically. Contour maps showing the

pore pressure in the saturated clay layer in the time domain have been plotted for the normal strip and normal line loading.

2. Theory

A homogeneous, isotropic, poroelastic medium with compressible fluid and solid constituents can be characterized by four poroelastic constants: the shear modulus (G), the drained Poisson's ratio (ν), the undrained Poisson's ratio (ν_u) and the Biot-Willis coefficient (α) as the basic set (Detournay and Cheng [16]). For plane strain deformation of a poroelastic medium in the x_1x_3 -plane, the displacement components in the solid skeleton are of the form

$$u_1 = u_1(x_1, x_3, t), u_2 = 0, u_3 = u_3(x_1, x_3, t). \tag{1}$$

Let σ_{ij} denote the total stress tensor in the fluid-infiltrated porous elastic material, ε_{ij} the corresponding strain tensor and p the excess fluid pore pressure. We take σ_{ij} and p as the basic state variables. For plane strain case, a suitable solution for the deformation of a homogeneous poroelastic clay stratum $0 \leq z \leq h$ is (Rani et. al.[14])

$$p = \int_0^\infty [A_1 e^{-mz} + A_2 e^{-kz} + A_3 e^{mz} + A_4 e^{kz}] \begin{pmatrix} \sin kx \\ \cos kx \end{pmatrix} dk, \tag{2}$$

$$F = \int_0^\infty [B_1 e^{-mz} + (B_2 + B_3 kz) e^{-kz} + B_4 e^{mz} + (B_5 + B_6 kz) e^{kz}] \begin{pmatrix} \sin kx \\ \cos kx \end{pmatrix} dk, \tag{3}$$

where now $p(x_1, x_3, s)$ and $F(x_1, x_3, s)$ denote the Laplace transforms of $p(x_1, x_3, t)$ and $F(x_1, x_3, t)$, respectively and s denotes the Laplace transform variable and the arbitrary constants A_1, A_2 , etc. may be functions of k , $x = x_1, z = x_3$,

$$m = \left(\frac{c_1}{c_3} k^2 + \frac{s}{c_3} \right)^{1/2} \tag{4}$$

and

$$\begin{aligned} B_1 &= \frac{2\eta}{k^2 - m^2} A_1, & B_4 &= \frac{2\eta}{k^2 - m^2} A_3. \\ B_3 &= \frac{\alpha_0 A_2}{2k^2 (\nu_u - \nu)} \left[1 + \frac{(c_1 - c_3)(1 - \nu_u)k^2}{(1 - \nu)s} \right], \\ B_6 &= -\frac{\alpha_0 A_4}{2k^2 (\nu_u - \nu)} \left[1 + \frac{(c_1 - c_3)(1 - \nu_u)k^2}{(1 - \nu)s} \right]. \end{aligned} \tag{5}$$

By Darcy's law, the fluid flux $\mathbf{q}(q_1, q_2, q_3)$ is given in a poroelastic medium with anisotropic permeability

$$q_1 = -\chi_1 \partial p / \partial x_1, \quad q_2 = 0, \quad q_3 = -\chi_3 \partial p / \partial x_3, \quad (6)$$

Using equation (2) and (6), we obtain

$$q_1 = -\chi_1 \int_0^\infty [A_1 e^{-mz} + A_2 e^{-kz} + A_3 e^{mz} + A_4 e^{kz}] \begin{pmatrix} \cos kx \\ -\sin kx \end{pmatrix} k \, dk, \quad (7)$$

$$q_3 = \chi_3 \int_0^\infty [m(A_1 e^{-mz} - A_3 e^{mz}) + k(A_2 e^{-kz} - A_4 e^{kz})] \begin{pmatrix} \sin kx \\ \cos kx \end{pmatrix} dk, \quad (8)$$

The stresses in term of Biot's stress function F are given by (Wang [17])

$$\sigma_{11} = \frac{\partial^2 F}{\partial x_3^2}, \quad \sigma_{33} = \frac{\partial^2 F}{\partial x_1^2}, \quad \sigma_{13} = -\frac{\partial^2 F}{\partial x_1 \partial x_3} \quad (9)$$

Using equation (3) and (9), we obtain

$$\sigma_{11} = \int_0^\infty \left[m^2 (B_1 e^{-mz} + B_4 e^{mz}) + k^2 \left\{ [B_2 + (kz - 2)B_3] e^{-kz} + [B_5 + (kz + 2)B_6] e^{kz} \right\} \right] \begin{pmatrix} \sin kx \\ \cos kx \end{pmatrix} dk, \quad (10)$$

$$\sigma_{33} = - \int_0^\infty \left[(B_1 e^{-mz} + B_4 e^{mz}) + (B_2 + B_3 kz) e^{-kz} + (B_5 + B_6 kz) e^{kz} \right] \begin{pmatrix} \sin kx \\ \cos kx \end{pmatrix} k^2 \, dk, \quad (11)$$

$$\sigma_{13} = \int_0^\infty \left[m(B_1 e^{-mz} - B_4 e^{mz}) + k \left\{ [B_2 + (kz - 1)B_3] e^{-kz} - [B_5 + (kz + 1)B_6] e^{kz} \right\} \right] \begin{pmatrix} \cos kx \\ -\sin kx \end{pmatrix} k \, dk. \quad (12)$$

Corresponding to the stresses given by equations (10)-(12) and integrating the constitutive equations

$$\begin{aligned} 2G\varepsilon_{11} &= (1 - \nu)\sigma_{11} - \nu\sigma_{33} + \alpha_0 p, \\ 2G\varepsilon_{33} &= (1 - \nu)\sigma_{33} - \nu\sigma_{11} + \alpha_0 p, \\ 2G\varepsilon_{13} &= \sigma_{13}, \end{aligned} \quad (13)$$

the displacements are found by

$$\begin{aligned} 2Gu_1 &= - \int_0^\infty \left[B_1 e^{-mz} + B_4 e^{mz} + \left\{ B_2 + B_3 (kz + 2\nu - 2) + \frac{\alpha_0}{k^2} A_2 \right\} e^{-kz} \right. \\ &\quad \left. + \left\{ B_5 + B_6 (kz - 2\nu + 2) + \frac{\alpha_0}{k^2} A_4 \right\} e^{kz} \right] \begin{pmatrix} \cos kx \\ -\sin kx \end{pmatrix} k \, dk, \end{aligned} \quad (14)$$

$$2Gu_3 = \int_0^\infty \left[m(B_1 e^{-mz} - B_4 e^{mz}) + \left\{ B_2 + B_3(1 - 2\nu + kz) - \frac{\alpha_0}{k^2} A_2 \right\} k e^{-kz} - \left\{ B_5 + B_6(1 - 2\nu - kz) + \frac{\alpha_0}{k^2} A_4 \right\} k e^{kz} \right] \begin{pmatrix} \sin kx \\ \cos kx \end{pmatrix} dk. \quad (15)$$

Equations (2), (7), (8), (10) to (12), (14) and (15) are the integral expressions for the deformation of a homogeneous poroelastic clay layer possessing anisotropic permeability and compressible constituents. The constants A_1, A_2, B_1, B_2 etc. are to be determined from the boundary conditions.

3. Surface loads

A normal load $(\sigma_{33})_0$ is applied on the surface $z = 0$ of the poroelastic clay stratum $0 \leq z \leq h$ overlying a smooth-rigid base (Figure 1). We assume that the boundary $z = 0$ is permeable, but the lower boundary $z = h$ may be permeable or impermeable. We consider both the cases: Case I, when the base $z = h$ is permeable and Case II, when the base $z = h$ is impermeable. The boundary conditions yield

$$\sigma_{13} = 0, \quad \sigma_{33} = (\sigma_{33})_0, \quad p = 0 \quad \text{at } z = 0, \quad (16)$$

and

$$\sigma_{13} = u_3 = p = 0 \quad \text{at } z = h \quad (17)$$

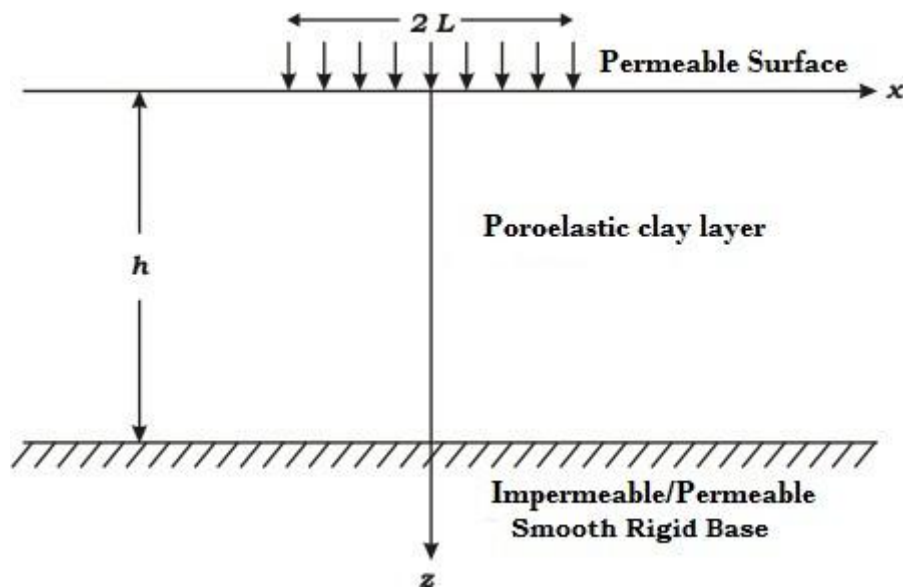


Figure 1. A poroelastic clay layer of thickness h with permeable surface overlying a smooth-rigid permeable or impermeable base.

for case I, and

$$\sigma_{13} = u_3 = q_3 = 0 \quad \text{at } z = h \quad (18)$$

for case II. Let

$$(\sigma_{33})_0 = \int_0^{\infty} N_0 \begin{pmatrix} \sin kx \\ \cos kx \end{pmatrix} k \, dk. \quad (19)$$

Applying the boundary conditions we obtain six equations in six unknowns ($A_1, A_2, A_3, A_4, B_2, B_5$) which are solved by Cramer's rule. Explicit expressions for these unknowns are given in Appendix A and B for Case I: Permeable base and Case II: Impermeable base, respectively.

Inserting the values of A_1, A_2 , etc. in equations (2), (7), (8), (10) to (12), (14) and (15), we get the integral expressions for the pore pressure, fluid flux, stresses and the displacements.

3.1 Normal strip loading

Consider a strip $-L \leq x \leq L$ of infinite length in the y -direction on the surface. Let a normal load σ_0 per unit length acting in the positive z -direction be uniformly distributed over this strip. We have (Singh and Rani [18])

$$(\sigma_{33})_0 = -\frac{\sigma_0}{\pi} \int_0^{\infty} \cos kx \frac{\sin kL}{kL} \, dk \quad (20)$$

for $z = 0$. Comparing equation (19) and (20), we have

$$N_0 = -\frac{\sigma_0}{\pi k} \begin{pmatrix} \sin kL \\ kL \end{pmatrix} \quad (21)$$

and the lower solution in equations (2), (7), (8), (10) to (12), (14) and (15) is to be chosen. Inserting the values of constants, A_1, A_2 , etc. from Appendix A and B into equations (2), (7), (8), (10) to (12), (14) and (15), we get the expressions for the pore pressure, fluid flux, stresses and displacements at any point of the stratum caused by strip loading for Case I: Permeable base and Case II: Impermeable base, respectively. We have verified that, as the depth h of stratum tends to ∞ , the integral expressions coincide with the corresponding results of a poroelastic half-space with anisotropic permeability and compressible constituents given by Singh *et al.* [19]. Explicit expressions for the pore pressure $p(x, z, s)$ and the vertical (down) displacement $u_3(x, z, s)$ are as follows:

Case I: Permeable base

$$p(x, z, s) = -\frac{\sigma_0}{\pi \eta s} \int_0^{\infty} \left[\left\{ 2(e^{kh} - e^{-kh}) - e^{(m+2k)h} + e^{(m-2k)h} \right\} e^{-mz} \right. \\ \left. + \left\{ e^{-mh} - e^{mh} + e^{(m+2k)h} - e^{-(m-2k)h} \right\} e^{-kz} + \left\{ 2(e^{-kh} - e^{kh}) - e^{-(m+2k)h} + e^{-(m-2k)h} \right\} e^{mz} \right]$$

$$+ \left\{ e^{mh} - e^{-mh} - e^{(m-2k)h} + e^{-(m+2k)h} \right\} e^{kz} \left] \frac{\sin kL \cos kx}{kLD'} dk, \quad (22)$$

$$\begin{aligned} u_3(x, z, s) = & \frac{\sigma_0}{2G\pi s} \int_0^\infty \left[mb_5 \left\{ 2(e^{kh} - e^{-kh}) - e^{(m+2k)h} + e^{(m-2k)h} \right\} e^{-mz} \right. \\ & - mb_5 \left\{ 2(e^{-kh} - e^{kh}) - e^{-(m+2k)h} + e^{-(m-2k)h} \right\} e^{mz} - \{ 2mb_5 (3e^{kh} + e^{-kh}) \\ & - (3mb_5 + b_4 - b_1 - b_2) e^{mh} - (3mb_5 - b_4 + b_1 + b_2) e^{-mh} - (mb_5 + b_4) e^{-(m-2k)h} \\ & - (mb_5 - b_4) e^{(m+2k)h} \} e^{-kz} + \{ 2mb_5 (3e^{-kh} + e^{kh}) - (3mb_5 - b_4 - b_1 - b_2) e^{mh} \\ & - (3mb_5 + b_4 + b_1 + b_2) e^{-mh} - (mb_5 + b_4) e^{(m-2k)h} - (mb_5 - b_4) e^{-(m+2k)h} \} e^{kz} \\ & \left. - (b_4 kz - b_3) \left\{ e^{-mh} - e^{mh} + e^{(m+2k)h} - e^{-(m-2k)h} \right\} e^{-kz} \right. \\ & \left. - (b_4 kz + b_3) \left\{ e^{mh} - e^{-mh} - e^{(m-2k)h} + e^{-(m+2k)h} \right\} e^{kz} \right] \frac{\sin kL \cos kx}{k^2 LD'} dk, \quad (23) \end{aligned}$$

Case II: Impermeable base

$$\begin{aligned} p(x, z, s) = & -\frac{\sigma_0}{\pi\eta s} \int_0^\infty \left[\left\{ e^{(m+2k)h} - e^{(m-2k)h} \right\} e^{-mz} \right. \\ & + \left\{ e^{mh} + e^{-mh} - e^{(m+2k)h} - e^{-(m-2k)h} \right\} e^{-kz} + \left\{ e^{-(m-2k)h} - e^{-(m+2k)h} \right\} e^{mz} \\ & \left. - \left\{ e^{mh} + e^{-mh} - e^{(m-2k)h} - e^{-(m+2k)h} \right\} e^{kz} \right] \frac{\sin kL \cos kx}{kLD} dk, \quad (24) \end{aligned}$$

$$\begin{aligned} u_3(x, z, s) = & \frac{\sigma_0}{2G\pi s} \int_0^\infty \left[mb_5 \left\{ e^{(m+2k)h} - e^{(m-2k)h} \right\} e^{-mz} - mb_5 \left\{ e^{-(m-2k)h} - e^{-(m+2k)h} \right\} e^{mz} \right. \\ & - \left\{ (mb_5 + b_4 - b_1 - b_2) e^{mh} - (mb_5 - b_4 + b_1 + b_2) e^{-mh} - (mb_5 + b_4) e^{-(m-2k)h} \right. \\ & + (mb_5 - b_4) e^{(m+2k)h} \} e^{-kz} + \left\{ (mb_5 - b_4 - b_1 - b_2) e^{mh} - (mb_5 + b_4 + b_1 + b_2) e^{-mh} \right. \\ & \left. + (mb_5 + b_4) e^{(m-2k)h} - (mb_5 - b_4) e^{-(m+2k)h} \right\} e^{kz} \\ & \left. - (b_4 kz - b_3) \left\{ e^{mh} + e^{-mh} - e^{(m+2k)h} - e^{-(m-2k)h} \right\} e^{-kz} \right. \\ & \left. + (b_4 kz + b_3) \left\{ e^{mh} + e^{-mh} - e^{(m-2k)h} - e^{-(m+2k)h} \right\} e^{kz} \right] \frac{\sin kL \cos kx}{k^2 LD} dk. \quad (25) \end{aligned}$$

3.2 Normal Line Loading

Suppose a normal line load σ_0 per unit length is applied at the origin on the surface $z = 0$ acting in the positive z -direction. Therefore

$$(\sigma_{33})_0 = -\frac{\sigma_0}{\pi} \int_0^\infty \cos kx dk \quad (26)$$

at $z = 0$. Comparing equation (19) and (26), we have

$$N_0 = -\frac{\sigma_0}{\pi k} \quad (27)$$

and the lower solution in equation (2), (7), (8), (10) to (12), (14) and (15) is to be chosen. The expressions for the pore pressure and vertical displacements can be obtained from the equation (22)-(25) by substituting the term $(\sin kL / kL) = 1$

4. Numerical Results and Discussion

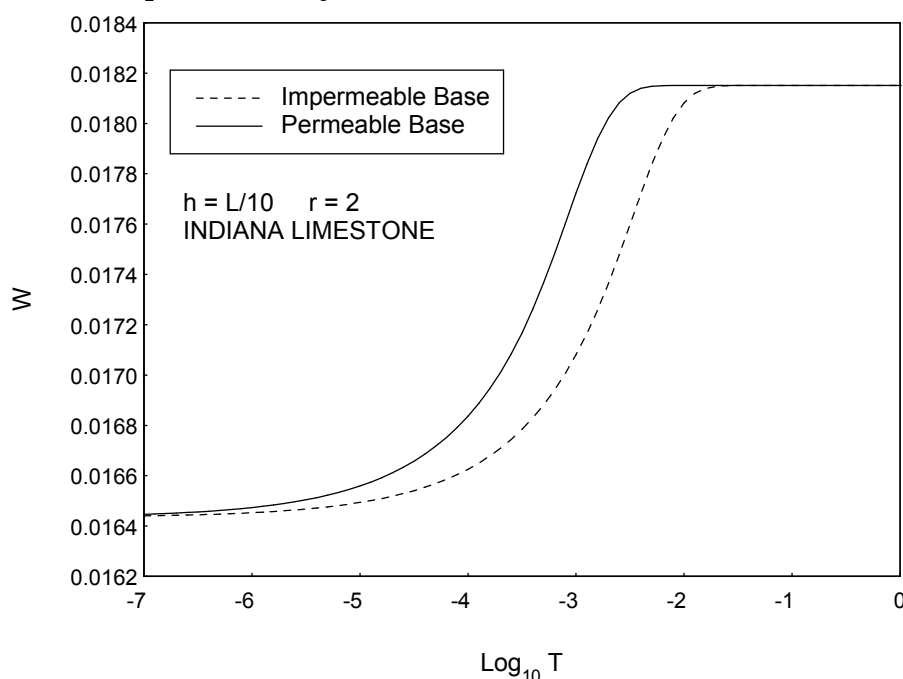
Equations (22)-(25) give the solution in the Fourier-Laplace transform domain. The double integral is evaluated numerically to obtain the solution in the space-time domain. We have used fixed Talbot Algorithm [20] for the Laplace inversion and the Fourier transform inversion has been evaluated by using the extended Simpson's rule.

We have computed the surface settlement u_3 and the pore pressure p at various points lying on the z -axis vertically below the origin. We define the following dimensionless quantities:

$$P = \left(\frac{L}{\sigma_0} \right) p, \quad W = \left(\frac{G}{\sigma_0} \right) u_3(0,0),$$

$$T = \frac{2G\chi_3 t}{L^2}, \quad r = \left(\frac{c_1}{c_3} \right)^{\frac{1}{2}} = \left(\frac{\chi_1}{\chi_3} \right)^{\frac{1}{2}}. \quad (28)$$

The petroleum deposits are found in structural traps between porous and non-porous rocks and the porous rocks are generally of Lime sandstone. Therefore, for numerical computations, we assume the poroelastic layer to be Indiana Limestone in which (Wang [17]) $\nu = 0.26, \nu_u = 0.33, \alpha = 0.71$. Also, the horizontal permeability is greater than the vertical permeability. Therefore, $r > 1$ and we take $r = 2$.



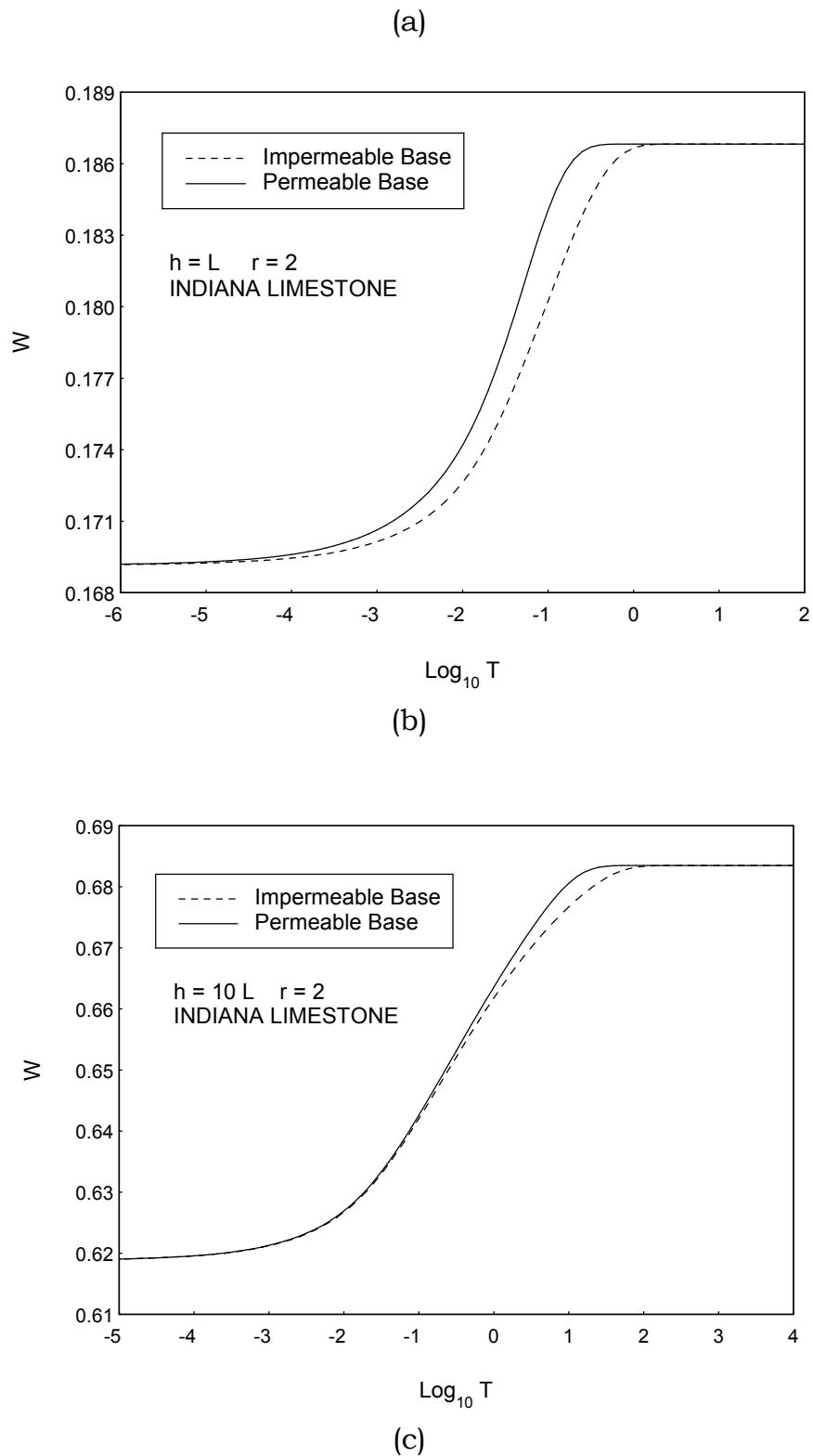


Figure 2. Effect of permeability of the base on the time settlement of the layer, taking the thickness of the layer (a) $h = L/10$ (b) $h = L$ (c) $h = 10L$. For a thin layer, the permeability of the base accelerates the consolidation, but for thick layer such behavior is not found.

In Figure 2, we compare the surface settlement W for permeable and impermeable base. Figure 2 displays the effect of permeability of the base on the surface settlement with time for $r = 2$ (a) $h = L/10$, (b) $h = L$ (c) $h = 10L$. The surface settlement is accelerated by the permeability of the base, without affecting the initial and the final settlement. For a thin layer, there is a significant effect of permeability of the base on the surface settlement.

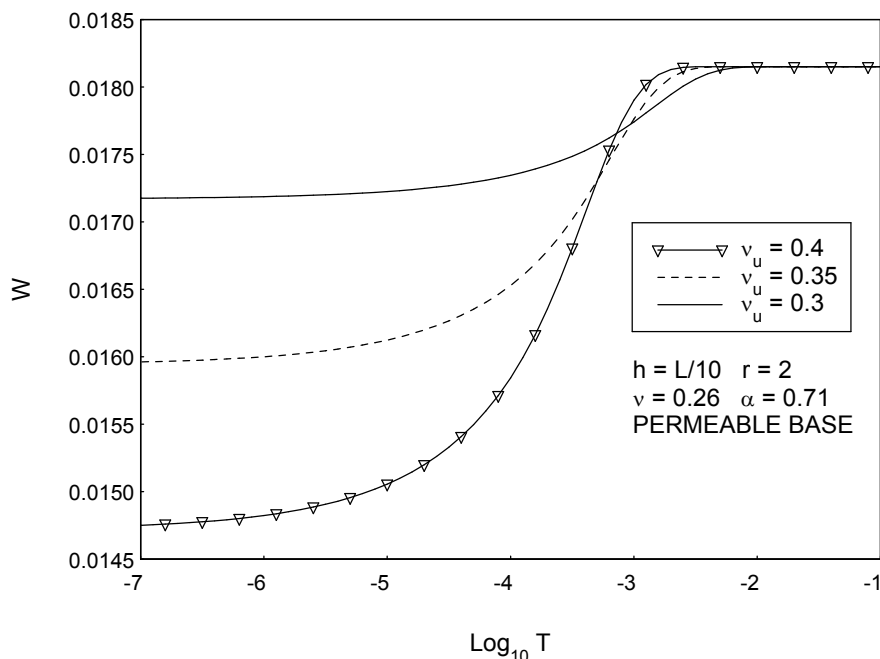


Figure 3. Effect of the compressibility of the pore fluid (v_u) on the time-settlement $W(0, 0, t)$ at origin for $\nu = 0.26, \alpha = 0.71$ and $r = 2$ for the layer thickness $h = L/10$.

Next, we compute the surface settlement W for permeable smooth-rigid base. The effect of undrained Poisson's ratio v_u ($-1 \leq \nu \leq v_u \leq 0.5$) on the surface settlement is shown in Figure 3 for $\nu = 0.26, \alpha = 0.71$ and $r = 2$ for $h = L/10$. We observe that the fluid constituent's compressibility decreases the initial undrained settlement but has no effect on the final drained settlement. Figure 4 shows the effect of Skempton's coefficient B ($0 \leq B \leq 1$) given by

$$B = \frac{3(v_u - \nu)}{\alpha(1 - 2\nu)(1 + v_u)},$$

on the time-settlement at the mid point ($x = z = 0$) of the strip ($-L \leq x \leq L$) for $\nu = 0.26, v_u = 0.33, r = 2$ for the stratum thickness $h = L/10$. The Skempton's coefficient $B = 1$ is for a poroelastic material with incompressible solid skeleton. We observe that the compressibility of the solid skeleton increases the surface consolidation.

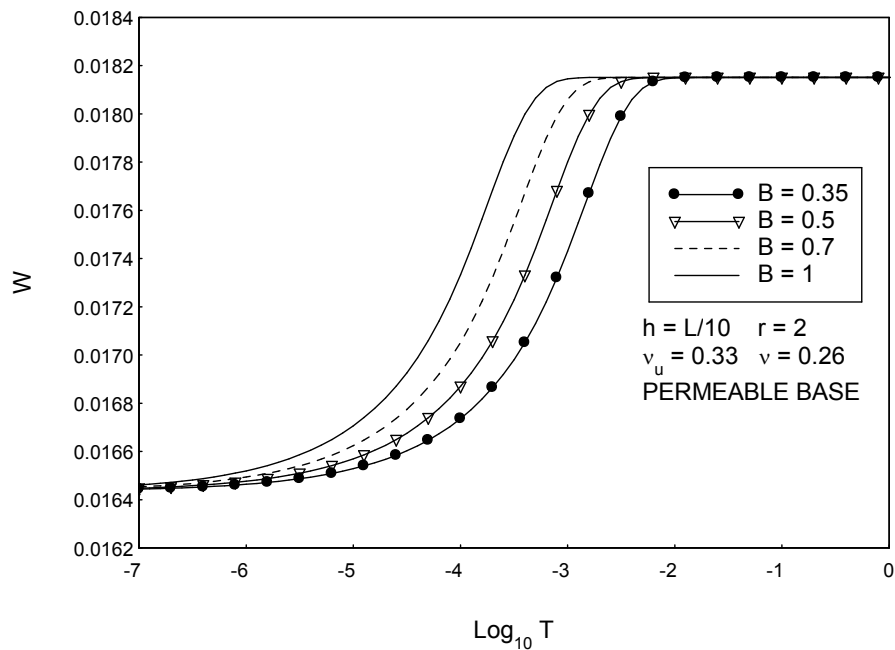


Figure 4. Effect of the compressibility of the solid skeleton (B) on the time-settlement $W(0, 0, t)$ at origin for $\nu = 0.26, \nu_u = 0.33$ and $r = 2$ for the layer thickness $h = L/10$.

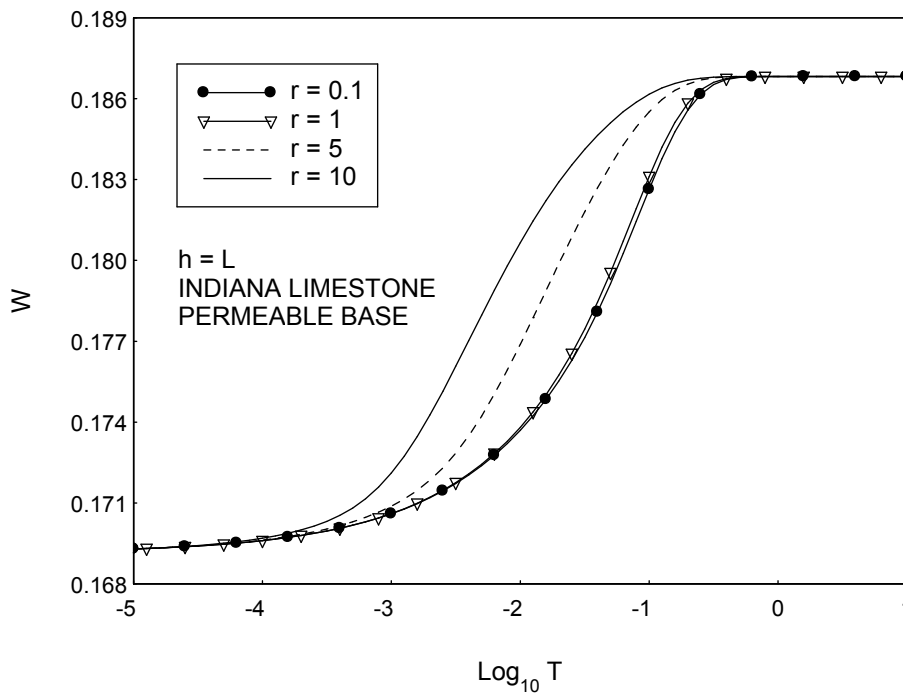


Figure 5. Effect of anisotropic permeability (r) on the surface settlement with time for permeable base. We observe that the settlement is faster for large value of anisotropic permeability (r).

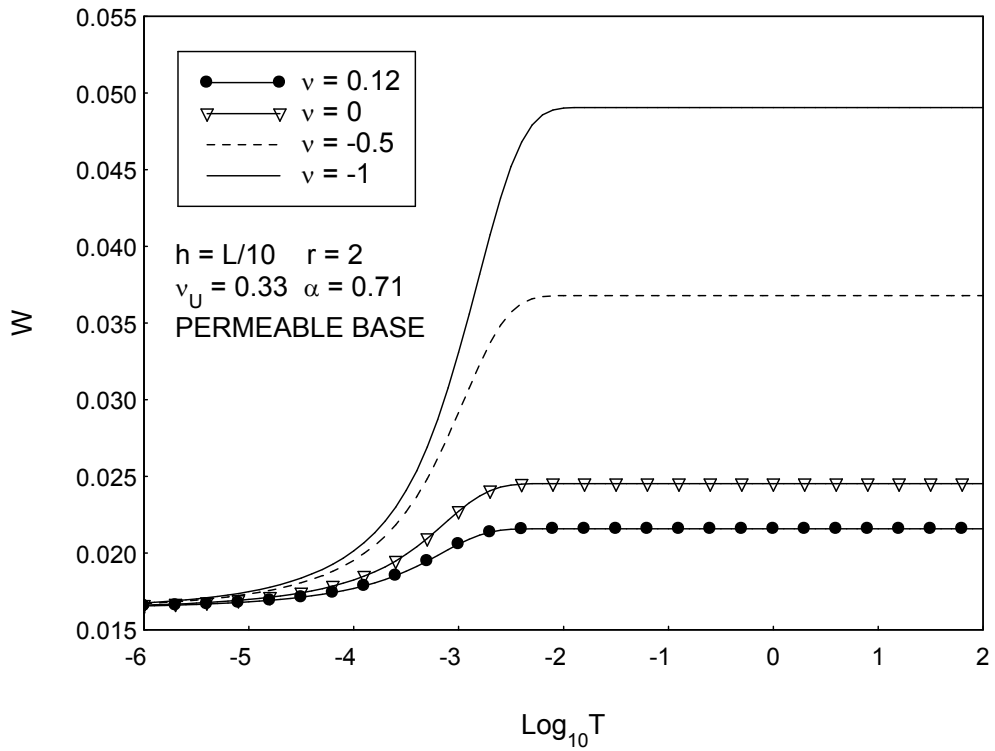
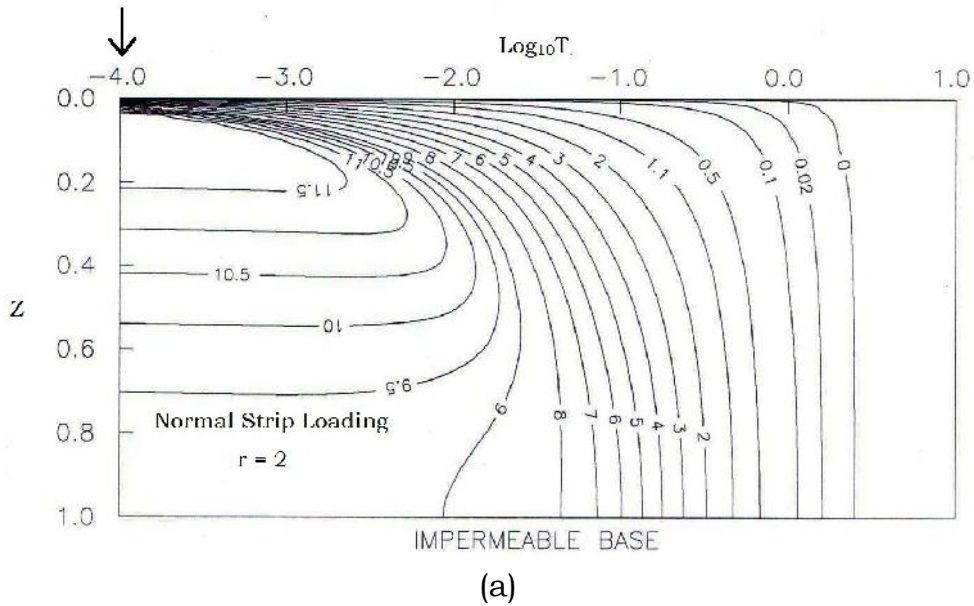


Figure 6. Time settlement of the layer for various values of v for the layer thickness $h = L/10$ for permeable base.



(a)

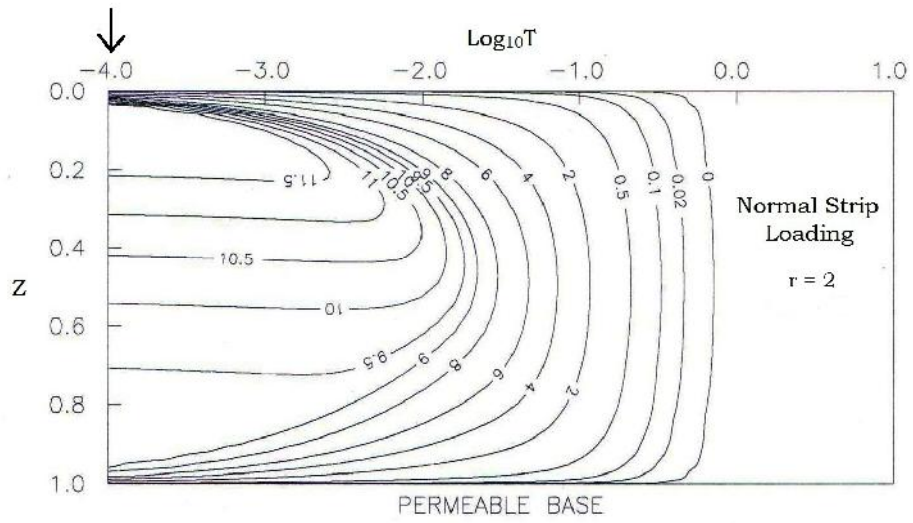
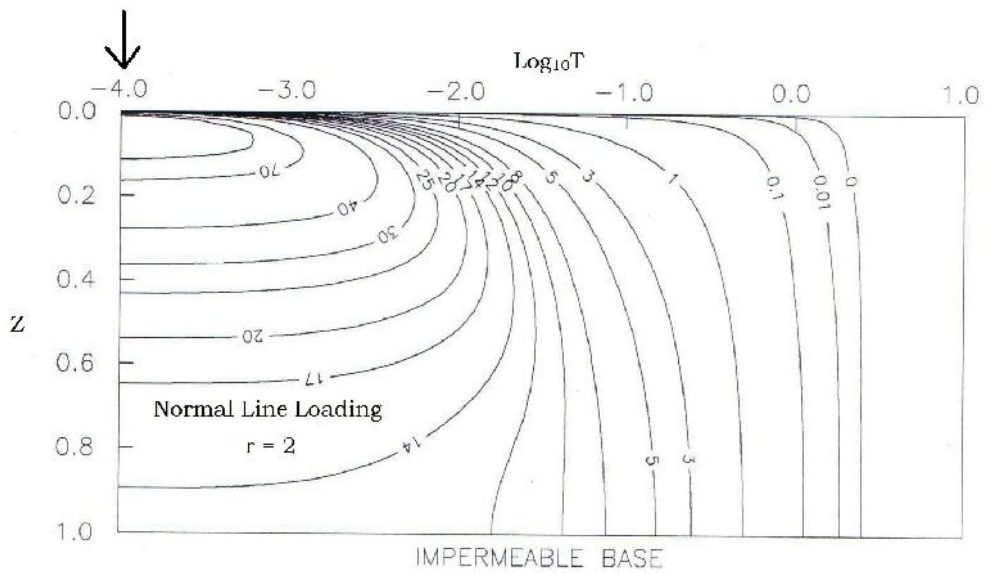
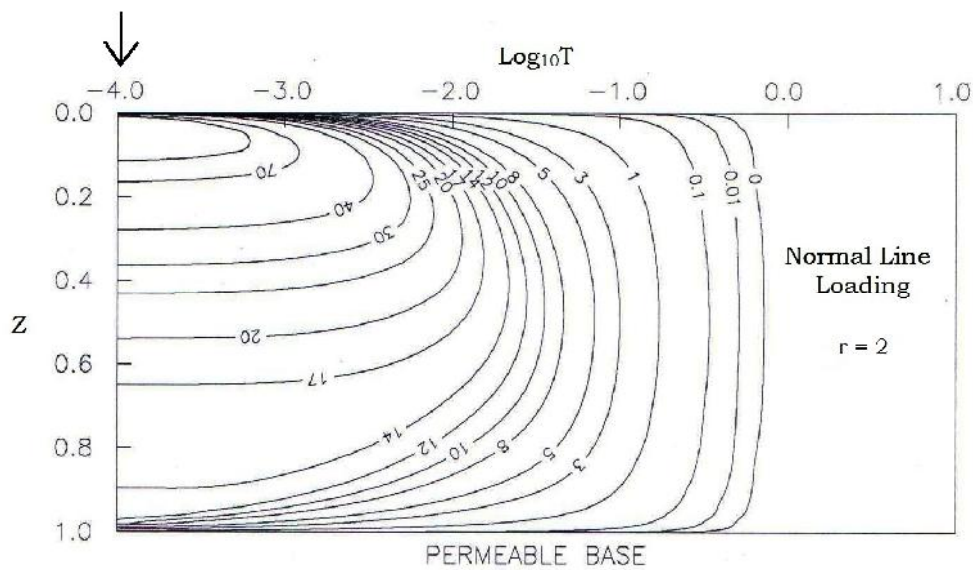


Figure 7. Diffusion of pore pressure P in the layer $0 \leq z \leq h$ with time at origin for normal strip loading for (a) Impermeable base (b) Permeable Base.





(b)

Figure 8. Diffusion of pore pressure P in the layer $0 \leq z \leq h$ with time at origin for normal line loading for (a) Impermeable base (b) Permeable Base. We observe that the magnitude of the pore pressure is increased due to line loading.

Figure 5 displays the effect of anisotropic permeability r for permeable base on the surface settlement with time. The settlement is faster for large value of anisotropic permeability (r). Figure 6 shows the effect of the Poisson's ratio ν with time on the time settlement of the layer for various values of ν . The negative Poisson's ratio increases the magnitude of surface settlement.

Contour maps showing the diffusion of pore pressure at origin in the poroelastic layer have been plotted with time. The pore pressure P is computed in units of $P \times 10^2$. The contour values for the isolines are indicated. The nodal lines are also drawn. Figure 7a exhibits the contour map of P for normal strip loading at the mid point of the strip for permeable base. Figure 7b is for impermeable base. We observe that the pore pressure vanishes more rapidly for the permeable base as compared to the impermeable base. Figure 8a shows the contour map of P for normal line loading for permeable base. Figure 8b is for impermeable base. The magnitude of the pore pressure is increased due to line loading. Diffusion of pore pressure with time is shown in figure 9a for various values of Poisson's ratio ν near the upper surface $z = L/10$. Figure 9b is for the diffusion of pore pressure at the mid-point of the layer $z = L/2$. The pore pressure increases from its initial value before decaying to zero for the negative Poisson's ratio.

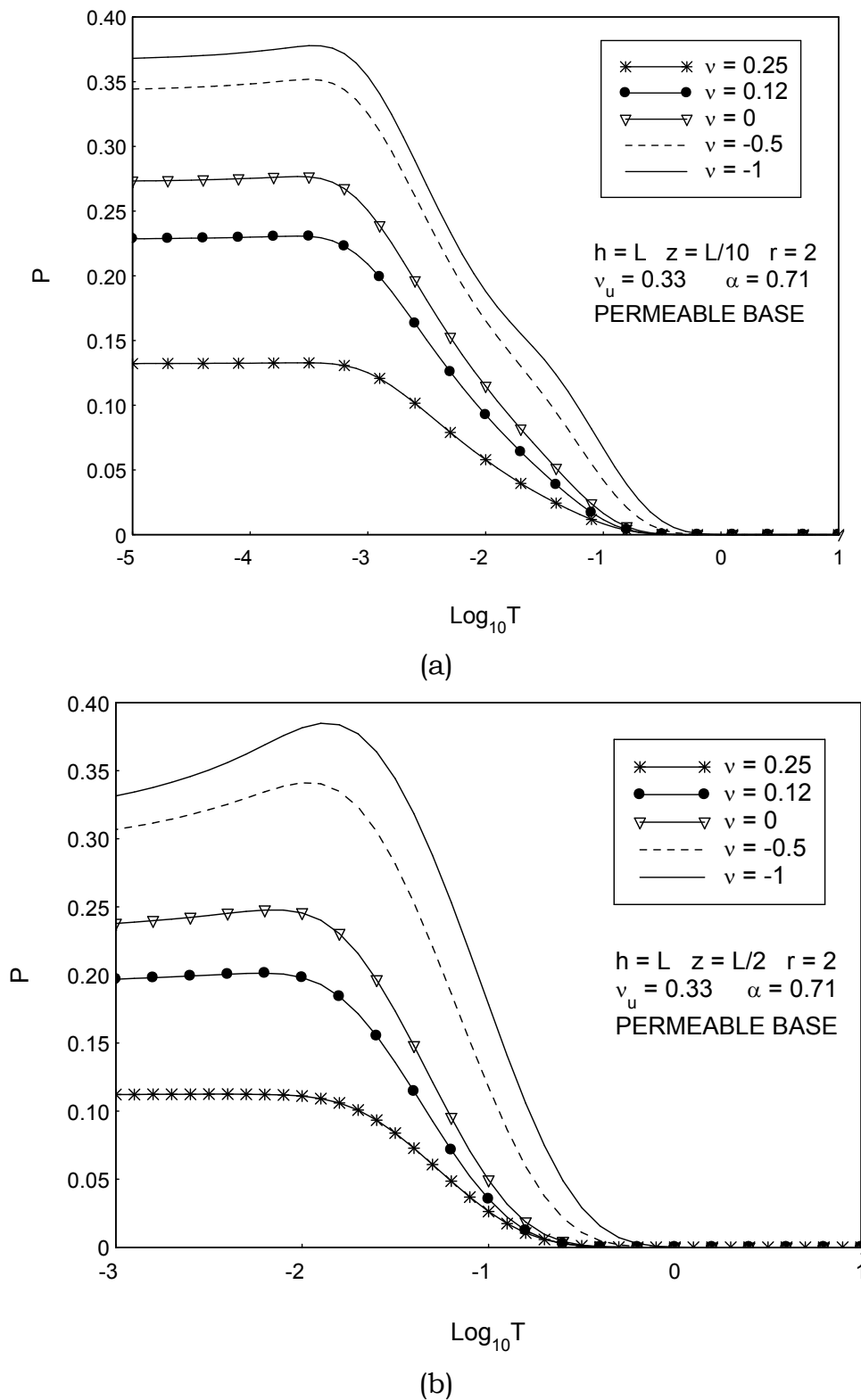


Figure 9. Diffusion of pore pressure P with time for various values of Poisson's ratio ν for $h = L$ for (a) $z = L/10$ (b) $z = L/2$. The Mandel-Cryer effect is observed for negative value of ν .

5. Conclusions

1. The permeability of the base accelerate the consolidation of the layer. For a thin layer, there is a significant effect of permeability of the base on the surface settlement. However, the initial and final surface settlement has no effect.
2. The compressibility of the solid skelton may accelerate the consolidation process without affecting the initial and final values of surface settlement.
3. The initial settlement is increased by the compressibility of the fluid constituents but there is no effect on the final settlement.
4. The pore pressure at origin vanishes more rapidly for the permeable base as compared to the impermeable base.
5. The pore pressure increases from its initial value before decaying to zero for the negative Poisson's ratio, which is Mandal Cryer effect.

References

- [1] Gibson R. E., Schiffman R. L. and Pu S. L., Plain strain and axially symmetric consolidation of a clay layer on a smooth impervious base, *Q. J. Mech. Appl. Math.*, **23**(1970), 505-520.
- [2] Booker J. R., The consolidation of a finite layer subject to surface loading, *Int. J. Solids Struct.* **10**(1974), 1053-1065.
- [3] Booker J. R. and Small J. C., Finite layer analysis of consolidation II, *Int. J. Numer. Anal. Meth. Geomech.*, **6**(1982),173-194.
- [4] Yue Z. Q. and Selvadurai A. P. S., Contact problem for saturated poroelastic solid, *J. Eng. Mech. ASCE*, **121**(1995),502-512.
- [5] Barry S. I., Mercer G. N. and Zoppou C., Deformation and fluid flow due to a source in poroelastic layer, *Appl. Math. Modelling*, **21**(1997),681-689.
- [6] Chen G. J., Steady state solutions of multilayered and cross-anisotropic poroelastic half-space due to a point sink, *Inter. J. Geomech.*, **5**(2005), 45-57.
- [7] Chen S L, Chen L Z and Zhang L M 2005a The axisymmetric consolidation of a semi-infinite transversely isotropic saturated soil. *Int. J. Numer. Anal. Meth. Geomech.* 29: 1249-1270
- [8] Chen S L, Zhang L M and Chen L Z 2005b Consolidation of a finite transversely isotropic soil layer on a rough impervious base. *J. Eng. Mech.* 131: 1279-1290
- [9] Ai Z Y and Wang Q S 2008 A new analytical solution to axisymmetric Biot's consolidation of a finite soil layer. *Appl. Math. Mech.* 29: 1617-1624
- [10] Singh S J, Kumar R and Rani S 2009 Consolidation of a poroelastic half-space with anisotropic permeability and compressible constituents by axisymmetric surface loading. *J. Earth Syst. Sci.* 118:563-574

- [11] Ai Z Y, Zeng W Z, Cheng Y C and Wu C 2011 Uncoupled state space solution to layered poroelastic medium with anisotropic permeability and compressible pore fluid. *Front. Archit. Civ. Eng. China* 5:171-179
- [12] Rani S, Kumar R and Singh S J 2011 Consolidation of an anisotropic compressible poroelastic clay layer by axisymmetric surface loads. *Inter. J. Geomech. ASCE* 11: 65-71
- [13] Ai Z Y, Cheng Y C, Zeng W Z and Wu C 2013 3-D consolidation of multilayered porous medium with anisotropic permeability and compressible pore fluid. *Mecca*. 48:491-499
- [14] Rani S, Puri M and Singh S J 2014 Plane strain consolidation of a compressible clay stratum by surface loads. *Geomech. Engg.* 7: 355-374
- [15] Rani S and Rani S Consolidation of an anisotropic soil stratum on a smooth-rigid base due to surface loads (Communicated)
- [16] Detournay E and Cheng A H D 1993 Fundamentals of poroelasticity. In: *Comprehensive Rock Engineering: Principles, Practice and Projects* (ed.) Hudson J A (Oxford: Pergamon Press) 2: 113-171.
- [17] Wang H F 2000 Theory of Linear Poroelasticity. (*Princeton: Princeton Univ. Press*).
- [18] Singh S J and Rani S 2006 Plane strain deformation of a multilayered poroelastic half-space by surface loads. *J. Earth Sys. Sci.* 115: 685-694
- [19] Singh S J, Rani S and Kumar R 2007 Quasi-static deformation of a poroelastic half-space with anisotropic permeability by two-dimensional surface loads. *Geophys. J. Int.* 170: 1311-1327
- [20] Talbot A 1979 The accurate inversion of Laplace transforms. *J. Inst. Maths. Applics.* 23: 97-120

Received: October 1, 2016

Appendix A

Case I: Permeable base

$$A_1 = \frac{N_0 k}{\eta D'} \left[2(e^{kh} - e^{-kh}) - e^{(m+2k)h} + e^{(m-2k)h} \right],$$

$$A_2 = \frac{N_0 k}{\eta D'} \left[e^{-mh} - e^{mh} + e^{(m+2k)h} - e^{-(m-2k)h} \right],$$

$$A_3 = \frac{N_0 k}{\eta D'} \left[2(e^{-kh} - e^{kh}) - e^{-(m+2k)h} + e^{-(m-2k)h} \right],$$

$$A_4 = \frac{N_0 k}{\eta D'} \left[e^{mh} - e^{-mh} - e^{(m-2k)h} + e^{-(m+2k)h} \right],$$

$$B_2 = \frac{N_0}{kD'} \left[2mb_5 (3e^{kh} + e^{-kh}) - (3mb_5 + b_4 - b_1 - b_2) e^{mh} - (3mb_5 - b_4 + b_1 + b_2) e^{-mh} \right. \\ \left. - (mb_5 + b_4) e^{-(m-2k)h} - (mb_5 - b_4) e^{(m+2k)h} \right],$$

$$B_5 = \frac{N_0}{kD'} \left[2mb_5 (3e^{-kh} + e^{kh}) - (3mb_5 - b_4 - b_1 - b_2) e^{mh} - (3mb_5 + b_4 + b_1 + b_2) e^{-mh} \right. \\ \left. - (mb_5 + b_4) e^{(m-2k)h} - (mb_5 - b_4) e^{-(m+2k)h} \right],$$

where

$$s_a = s + (c_1 - c_3)k^2 = c_3(m^2 - k^2)$$

$$b_1 = b_4kh - b_3, \quad b_2 = b_4kh + b_3,$$

$$b_3 = 1 - \frac{(1-2\nu)(1-\nu_u)s_a}{(\nu_u - \nu)s}, \quad b_4 = 1 + \frac{(1-\nu_u)s_a}{(\nu_u - \nu)s},$$

$$b_5 = \frac{2k}{m^2 - k^2},$$

and

$$D' = -8mb_5(e^{kh} + e^{-kh}) + 2(3mb_5 - b_1 - b_2)e^{mh} + 2(3mb_5 + b_1 + b_2)e^{-mh} \\ - [b_4 - (m-k)b_5][e^{(m+2k)h} + e^{-(m+2k)h}] + [b_4 + (m+k)b_5][e^{(m-2k)h} + e^{-(m-2k)h}],$$

Appendix B

Case II: Impermeable base

$$A_1 = \frac{N_0k}{\eta D} [e^{(m+2k)h} - e^{(m-2k)h}],$$

$$A_2 = \frac{N_0k}{\eta D} [e^{mh} + e^{-mh} - e^{(m+2k)h} - e^{-(m-2k)h}],$$

$$A_3 = \frac{N_0k}{\eta D} [e^{-(m-2k)h} - e^{-(m+2k)h}],$$

$$A_4 = \frac{N_0k}{\eta D} [-e^{mh} - e^{-mh} + e^{(m-2k)h} + e^{-(m+2k)h}],$$

$$B_2 = \frac{N_0}{kD} [(mb_5 + b_4 - b_1 - b_2)e^{mh} - (mb_5 - b_4 + b_1 + b_2)e^{-mh} - (mb_5 + b_4)e^{-(m-2k)h} \\ + (mb_5 - b_4)e^{(m+2k)h}],$$

$$B_5 = \frac{N_0}{kD} [(mb_5 - b_4 - b_1 - b_2)e^{mh} - (mb_5 + b_4 + b_1 + b_2)e^{-mh} + (mb_5 + b_4)e^{(m-2k)h} \\ - (mb_5 - b_4)e^{-(m+2k)h}],$$

where

$$D = -2(mb_5 - b_1 - b_2)e^{mh} + 2(mb_5 + b_1 + b_2)e^{-mh} \\ + [b_4 - (m-k)b_5][e^{(m+2k)h} - e^{-(m+2k)h}] + [b_4 + (m+k)b_5][e^{-(m-2k)h} - e^{(m-2k)h}],$$